PAPER

Contact resistivity due to oxide layers between two REBCO tapes

View the article online for updates and enhancements.

Contact resistivity due to oxide layers between two REBCO tapes

Jun Lu[1] , **Yan Xin**[1], **Eric Lochner**[2], **Kyle Radcliff**[1] **and Jeremy Levitan**[1]

[1] National High Magnetic Field Laboratory, Tallahassee, FL 32310, United States of America
[2] Department of physics, Florida State University, Tallahassee, FL 32306, United States of America

E-mail: junlu@magnet.fsu.edu

Abstract

In a no-insulation (NI) REBCO magnet, the turn-to-turn contact resistivity (ρ_c) determines its quench self-protection capability, charging delay time and the energy loss during field ramps. Therefore it is critically important to be able to control a range of ρ_c values suitable for various NI magnet coils. In this work, we investigate two possibilities to control ρ_c: by controlling the oxide layer of the copper surface of REBCO tapes; and by controlling the oxide layer in stainless steel co-wind tapes. We used a commercial oxidizing agent Ebonol® C to treat the copper surface of REBCO tapes. The copper oxide layer was characterized by cross-sectional transmission electron microscopy (TEM) and x-ray photoelectron spectroscopy (XPS). The oxide layer formed in Ebonol® C at 98 °C for 1 min is Cu_2O of 0.5–1 μm. The ρ_c between two oxidized REBCO is in the order of 35 mΩ cm^2 at 4.2 K which decreases to 10 mΩ cm^2 after 30 000 contact pressure cycles. The ρ_c increases but only by 5% at 77 K. We also investigated the effect of oxidation of stainless steel co-wind tape on ρ_c. The native oxides on 316 stainless steel tape as well as those heated in air at 200 °C–600 °C were examined by TEM and XPS. The native oxides layer is about 3 nm thick. After heating at 300 °C for 8 min and 600 °C for 1 min, its thickness increases to about 10 and 30 nm respectively. For the stainless steel tapes with about 10 nm surface oxides, pressure cycling for 30 000 cycles decreases ρ_c by almost 4 orders of magnitude. Whereas at 77 K, it only decreases by a factor of 3. For a surface with 30 nm oxide, the ρ_c decreases moderately with load cycles. The results suggest that for an oxidized stainless steel to achieve stable ρ_c over large number of load cycles a relatively thick oxide film is needed.

Keywords: REBCO, no-insulation, contact resistance, oxides, TEM, XPS

(Some figures may appear in colour only in the online journal)

1. Introduction

The no-insulation (NI) REBCO magnet has advantages of self-quench-protection and high engineering current density over its insulated counterpart [1–4]. But it also has a few significant drawbacks, such as long charging/discharging delays and high ramp losses, which limit its applications in user magnet systems where frequent field ramps are required. In addition, high transient electrical currents during a magnet quench result in high electromagnetic stresses that could damage the magnet [5]. All these drawbacks can be largely mitigated by increasing coils' turn-to-turn contact resistivity ρ_c. On the other hand, a very high ρ_c compromises the coil's self-quench-protection ability and results in magnet burn-out during a quench. Since the optimal ρ_c is coil specific, it is highly desirable to develop a technology to control ρ_c in a wide range.

Contact resistivity ρ_c have been measured in short samples and NI REBCO coils by a number of research groups [6–9]. Previously we measured ρ_c of short samples at 77 K and 4.2 K under different contact pressures [6]. The control of ρ_c by coating the surface of REBCO tapes with various materials has been attempted; and the effect of cyclic contact pressure was studied [7]. But a technique that reliably controls a wide range of ρ_c values which is consistent over a large number of pressure cycles is yet to be developed.

The theory of electrical contact resistance has been well established [10, 11]. For a contact with a thin resistive film, ρ_c

can be written as

$$\rho_c = \frac{\rho}{2aN} + \frac{\rho_f d}{\pi a^2 N}, \qquad (1)$$

where ρ and ρ_f are bulk resistivity of the base material and the film respectively; a and N are respectively the average radius and number density of contact asperity spots; d is the thickness of the resistive film. The first term represents the constriction resistance of the base material. The second term is the contribution from the resistive film. In principle, ρ_c can be controlled by changing the thickness d and resistivity ρ_f of the film. In practice though, a and N are unknown, and ρ_f at low temperatures is also difficult to control. So equation (1) can only provide a general guidance for ρ_c control. A reliable ρ_c control method will have to be developed largely by trial and error.

Copper surface exposed to ambient environment has a layer of native oxides which is only a few nanometers thick containing Cu_2O and CuO [12, 13], both semiconductors and highly resistivity at low temperatures [11, 14, 15]. But due to the thin thickness of the native oxides layer, the ρ_c of as received REBCO tapes whose contact is via copper stabilizer layer is low, in the order of 10^{-5} $\Omega\,cm^2$ at 77 and 4.2 K [6]. The existence of the native oxide is consistent with the considerable decrease in ρ_c of REBCO tapes at 77 K after 20 000 pressure cycles, which was interpreted as wearing/penetration of the native oxide layers [7].

In order to obtain a higher ρ_c, a thicker oxide layer is needed. Copper oxide growth by heating copper in air does not seem to be a good option. Because the oxide growth rate is very low below 200 °C, while heating REBCO tapes at above 200 °C causes critical current degradation [16]. A better option would be surface treatment by an oxidizing chemical agent at a temperature well below 200 °C. It is known that copper surface can be oxidized by a solution of sodium hydroxide (NaOH) and sodium nitrite ($NaClO_2$) at elevated temperatures [17, 18]. This process has been commercialized, and a copper blackening chemical called Ebonol® C is commercially available at Enthone Inc. The exact reaction chemistry between copper and Ebonol® C is not very clear. It was used to treat NbTi Rutherford cables in order to increase inter-strand contact resistance and reduce ac losses [19, 20]. It was also proposed to be used to treat REBCO tapes to increase ρ_c for NI magnet applications [21, 22].

Another method to control ρ_c in a NI magnet is to control the surface oxides on co-wind tapes. Since high field REBCO magnets often require co-wind tapes for mechanical reinforcement [4, 23], it is convenient to control the surface of co-wind tapes instead of that of the REBCO tapes. This way, the potential damage to the REBCO tapes during handling and the oxidation process is avoid. Compared with the damages to co-wind tapes, the damages to REBCO tapes are much more difficult to identify and much more expensive to replace.

Austenitic stainless steels also have a thin layer of native oxides in ambient environment, which is 2–3 nm thick [24]. The native oxides layer consists of Cr_2O_3, Fe_2O_3 and Fe_3O_4 [25]. Upon heating in air, the oxide layer becomes thicker and

its composition changes slightly as well [26]. The stainless steel tapes received from different manufacturers can have very different surface conditions depending on the details of the manufacturing process. This may partially explain the considerable difference in ρ_c reported by different groups [7, 27, 28]. Evidently surface oxides and their effects on ρ_c is critically important, but they have not been characterized in the context of ρ_c control.

In this paper, we characterized the oxide layers on REBCO tapes treated by Ebonol® C and on 316 stainless steel by heating in air by using transmission electron microscopy (TEM) and x-ray photoelectron spectroscopy (XPS). The ρ_c of these oxidized samples were measured at 77 K and 4.2 K under contact pressure up to 25 MPa and pressure cycles up to 30 000.

2. Experimental

The REBCO tape is SuperPower SCS4050 which has 20 μm plated copper stabilizer. 20% Ebonol® C special (Enthone Inc.) solutions were used to oxidize the copper surface of REBCO tapes. The oxidation was at 98 °C. For copper oxide growth rate studies, we used C110 copper stamp samples of about $12.7 \times 15 \times 0.5$ mm^3. Their cold-rolled surfaces were slightly polished by a Scotch-Brite pad. Each sample was weighed before and after oxidation, then weigh again after the oxide was removal by a 3.7% HCl solution for 2 min. The 3.7% HCl does not etch copper as verified by our experiments. A Mettler-Toledo Analytical balance XS104 (max. 120 g, precision 0.1 mg) was used to weigh the samples. The weight losses were used to calculate the oxides thickness. In the calculation, 6.0 and 8.96 g cm^{-3} were used for densities of Cu_2O and Cu respectively.

The stainless steel tape samples are type 316. They are 4 mm wide and 50 μm thick and in full-hard condition. Since the initial surface condition of the stainless steel tapes is unknown, all the as-received samples were etched by 37% HCl for 5 min to remove the initial surface oxides and reset the surface condition. Subsequently the stainless steel tape samples were heat treated in air at temperatures between 200 °C and 600 °C in a horizontal quartz tube furnace.

The oxidized surfaces of both REBCO and stainless steel were characterized by TEM and XPS. The TEM was performed using a JEOL JEM-ARM200cF, which is a probe-aberration-corrected microscope with a cold field emission electron gun operating at 200 kV. It is also equipped with a Gatan Quantum electron energy loss spectroscopy (EELS) spectrometer and an Oxford X-max silicon drift detector for energy dispersive spectroscopy (EDS). The cross-sectional TEM specimen of an oxidized REBCO tape was made by mechanical grinding/polishing and Ar ion milling. The cross-sectional TEM samples of oxidized stainless steel was cut by the Ga$^+$ focused ion beam in a Helios NanoLab dual beam scanning electron microscope (SEM). The XPS was performed in a Perkin-Elmer PHI-5100 system with Al $K\alpha$ x-ray energy of 1486.6 eV. The system has an Ar ion milling capability suitable for depth profile analysis. Ar ion source

was 3 kV for experiments in this paper. The contact resistivity were measured using the four-probe method with 1 A current on two identical short samples with a 25 mm overlap at both 77 and 4.2 K under cyclic contact pressure. Further details are described in our previous paper [7]. For stainless steel tape ρ_c measurements, the sample was sandwiched between two as-received REBCO tapes. So the reported ρ_c values are the sum of two stainless steel/REBCO interfaces.

3. Results and discussions

3.1. Ebonol® C treatment of REBCO surface

We measured oxide thickness as a function of treatment time in 20% Ebonol® C solution at 98 °C. The results are plotted in figure 1(a). The oxide growth follows a power law of time with an index of 0.6–0.8 (the inset of figure 1(a)). The original Ebonol® C solution is colorless. It turned to blue color after reaction with copper. This suggests that in the oxidizing process some copper is dissolved in the solution in the form of Cu(II) ions which is blue. This is consistent with the loss of copper also shown in figure 1(a). Obviously Ebonol® C treatment consumes a small fraction of the copper stabilizer. For a 20 μm stabilizer layer with a 1 μm oxide layer, the reduction of the stabilizer is not significantly. The effect of Ebonol® C treatment temperature and solution concentration are shown in figures 1(b) and (c) respectively. As expected, oxide thickness monotonically increases with both treatment temperature and Ebonol® C concentration.

Figure 2(a) is a cross-sectional TEM bright field image of the oxide layer on the REBCO tape treated by 20% Ebonol® C solution at 98 °C for 60 s. It shows a rough surface which is slightly less rough than the original plated copper surface of the untreated REBCO tape. There is a fine grain layer of 0.5–1 μm on top of the larger grained Cu. Combined elemental EDS maps of oxygen and Cu is shown in figure 2(b) confirmed that the fine grain layer is the oxide layer and the larger grains belong to the copper stabilizer. Selected area electron diffraction pattern (figure 2(c)) from one grain in the oxide layer was indexed to be a Cu_2O [101]. The extra diffraction spots around the main spots in figure 2(c) are from Cu [101] and their double diffractions. This results were reproduced on several other fine grains, which indicates that the oxide layer is mostly Cu_2O. The fine structure of Cu $L_{2,3}$ core-loss EELS spectrum from the oxide layer shown in figure 2(d) confirms that Cu in the oxide layer is Cu^{1+} [29], which is consistent with the Cu_2O phase.

The Ebonol® C treated sample was also studied by XPS where Cu $2p$ and O $1s$ peaks were scanned after different durations of Ar milling. The Ar milling rate of Cu_2O was not calibrated. After 400 min of Ar milling, sufficiently thick layer of oxide still remained as indicated by strong O $1s$ peak and the fact the surface was still black color. Figure 3 shows the Cu $2p$ spectra of the oxide layer. The Cu $2p_{3/2}$ peak near 932.5 eV is consistent with that of Cu_2O, different from Cu $2p_{3/2}$ of CuO at 933.7 eV [30]. Furthermore, Cu $2p$ of CuO has strong satellite peaks between 943 and 962 eV, which is
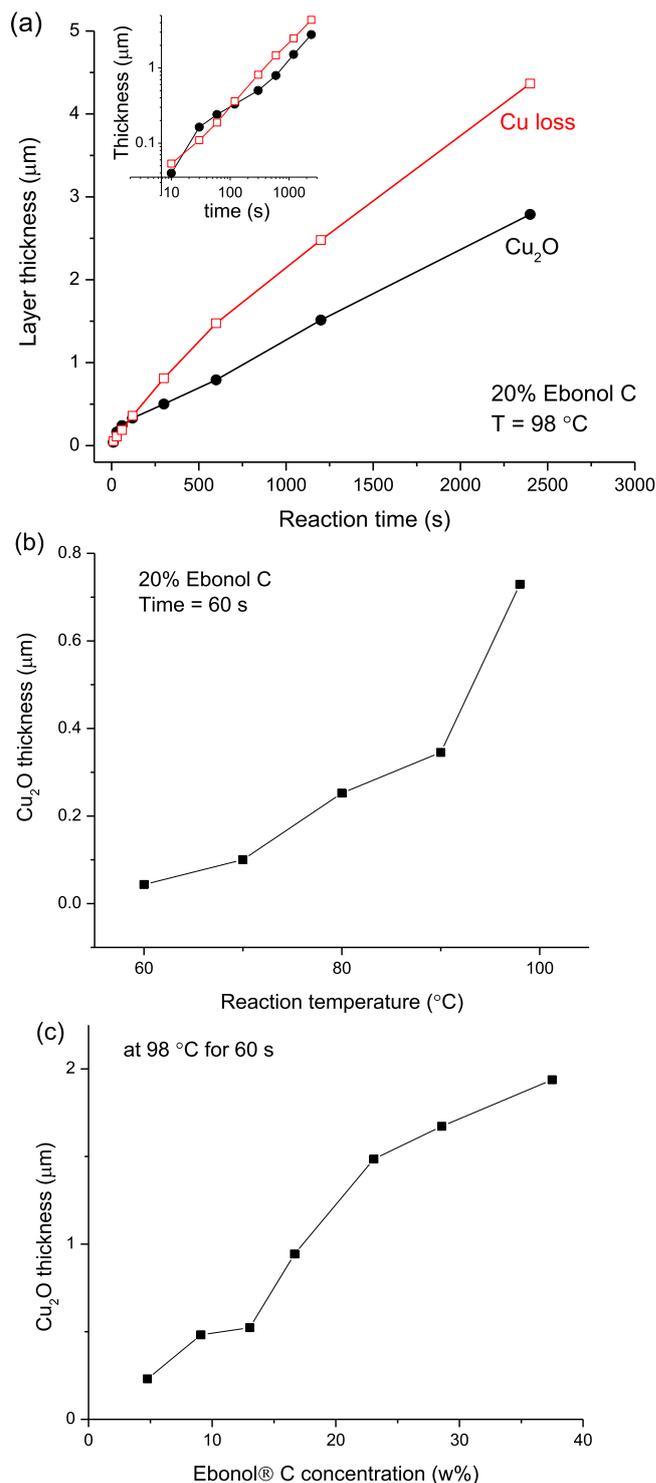
Figure 1. The thickness of Cu_2O on Cu stamp samples treated in Ebonol® C special solution (a) as a function of treatment time at 98 °C in 20% solution. The copper thickness loss is also plotted. The inset is a log–log plot of the same data. (b) as a function of reaction temperature for 1 min treatment in 20% solution (c) as a function of concentration at 98 °C for 1 min treatment.

absent in this spectrum. So these results confirm that the oxide layer is Cu_2O.

[7] The ρ_c versus pressure cycles of a sample treated by Ebonol® C at 98 °C for 1 min was measured at 4.2 K. The
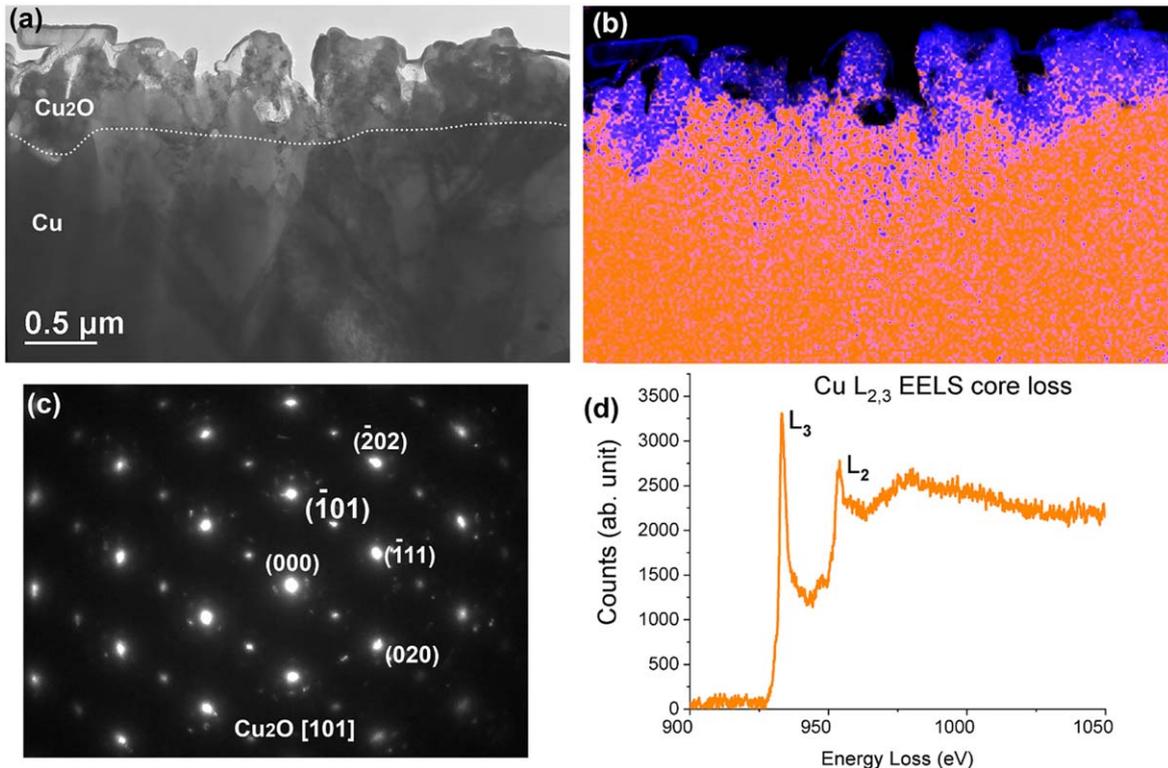
Figure 2. Cross-sectional TEM results of the oxide layer on a REBCO tape treated by Ebonol® C at 98 °C for 1 min. (a) Bright field image, the thin dashed line indicate the boundary between the fine grained top layer and the large gained substrate. (b) A combined EDS elemental map of Cu (orange) and O (blue) indicating that the top fine grained layer is copper oxide. (c) The electron diffraction pattern from a grain in the oxide layer. The main spots are from Cu_2O [101]. The extra spots are from Cu [101] and the double diffractions. (d) EELS spectrum of Cu $L_{2,3}$ core-loss from the oxide layer, which is consistent with Cu_2O spectrum.
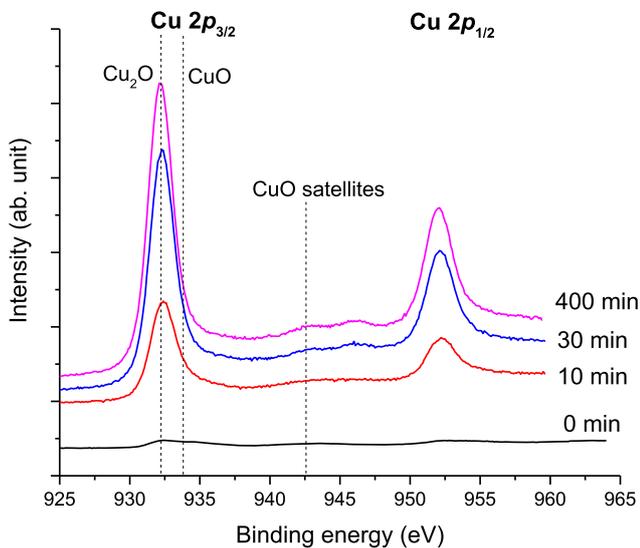
Figure 3. XPS Cu 2*p* spectra of REBCO tape surface oxidized by Ebonol® C for 1 min at 98 °C. The surface Ar milling time is indicated at each spectrum. The vertical dashed lines indicate the peak positions of Cu 2*p* of Cu_2O and CuO according to [30].

Figure 4. ρ_c versus pressure cycles of a REBCO tape treated by Ebonol® C for 1 min at 98 °C measured at 4.2 K under 25 MPa pressure. The cyclic contact pressure was 2.5–25 MPa.

results are shown in figure 4. ρ_c decreases with increasing pressure (not shown) similar to what have been observed in references [6] and [7]. There is a monotonic gradual decrease in ρ_c with number of cycles. At the end of 30 000 cycles, ρ_c is reduced by a factor of 3. The ρ_c of this sample is not temperature sensitive. Because when the temperature increased from 4.2 to 77 K, ρ_c only increased about 5% (data are not shown).

In order to demonstrate the feasibility of large scale oxidation of REBCO tapes, a reel-to-reel Ebonol® C oxidation system was designed and built. A photograph of the
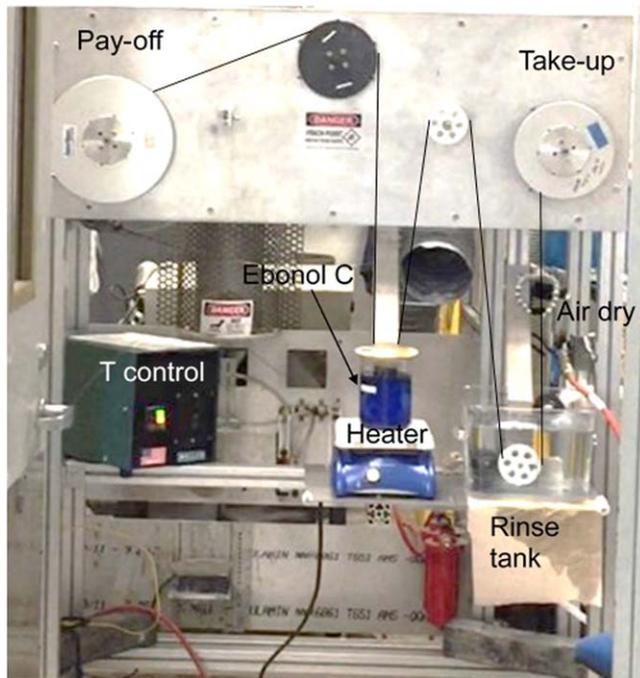
Figure 5. The reel-to-reel Ebonol® C oxidation treatment system.

Figure 6. ρc of a 316 stainless steel tape as a function of exposure time in laboratory environment after 5 min etch by 37% HCl. In the measurement, the stainless steel sample was sandwiched between two REBCO tapes. ρ_c was measured at 77 K under 25 MPa contact pressure after 5 pressure cycles of 2.5–25 MPa.

Figure 7. ρc of stainless steel tape samples at 77 K under 25 MPa pressure as a function of heat treatment temperature. The heat treatment time was 1 min.

system is shown in figure 5. The center of the system is an Ebonol® C solution container where oxidization reaction takes place. In addition to the solution temperature control and the tape speed control sub-systems, a water tank and two air nozzle are used to rinse off residual chemicals and dry the tape respectively after the oxidation. Our preliminary results showed that surface preparation, accurate and stable speed and temperature control are the keys in getting uniform copper oxide layer along the length. At the time of writing this paper, total of 400 meter of SuperPower REBCO tapes have been oxidized to be used in various test coils.

3.2. Surface oxides on stainless steel co-wind tape

The native oxides on stainless steel surface strongly influence its ρ_c. For our samples in as received condition, a ρ_c in the order of 100 000 $\mu\Omega\,\mathrm{cm}^2$ was measured at 77 K under 25 MPa pressure [7]. When they were slightly polished with a Scotch-Brite pad, however, ρ_c reduced dramatically to about 2400 $\mu\Omega\,\mathrm{cm}^2$. Similarly, when etched by concentrated (37%) HCl for 5 min at room temperature, ρ_c was reduced from dramatically from ~100 000 to ~1000 $\mu\Omega\,\mathrm{cm}^2$. Subsequently, the HCl etched samples were stored in air-conditioned lab environment for up to 4 months and their ρ_c were measured at 77 K. The ρ_c versus storage time is plotted in semi-log scale in figure 6. Despite the scatter, the data show that ρ_c increased very slowly with storage time. After 4 months of storage, ρ_c was still lower than 3000 $\mu\Omega\,\mathrm{cm}^2$, much lower than 100 000 $\mu\Omega\,\mathrm{cm}^2$ of the samples in as-received condition. This experiment implies that the native oxides formed in lab environment was very thin and nearly self-passivating. In contrast, the oxide layer formed in the manufacturing environment seems to be significantly thicker.
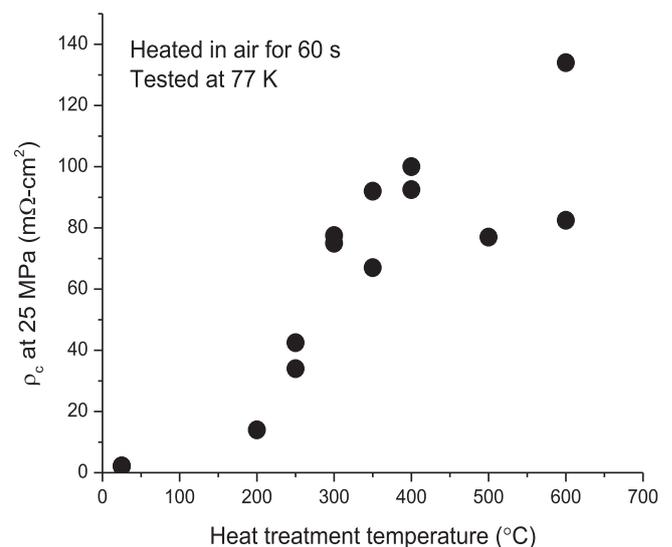
Apparently in order to increase ρ_c of stainless steel, a thicker oxide layer is needed. We heated a number of samples in air and studied their oxide layer. When heated between 200 °C and 600 °C, the color of the stainless steel surface changed due to the light interference from the oxides of different thicknesses consistent with reference [31]. ρ_c of the heat treated samples were measured at 77 K under 25 MPa pressure. As shown in figure 7, ρ_c increases with heat treatment temperature initially, but seems to level off above 400 °C.

The cross-sections of oxide layers are shown in figure 8. It includes annular dark field scanning transmission electron microscopy (ADF-STEM) images and EDS oxygen maps of samples heated for 8 min at 300 °C ((a), (c))
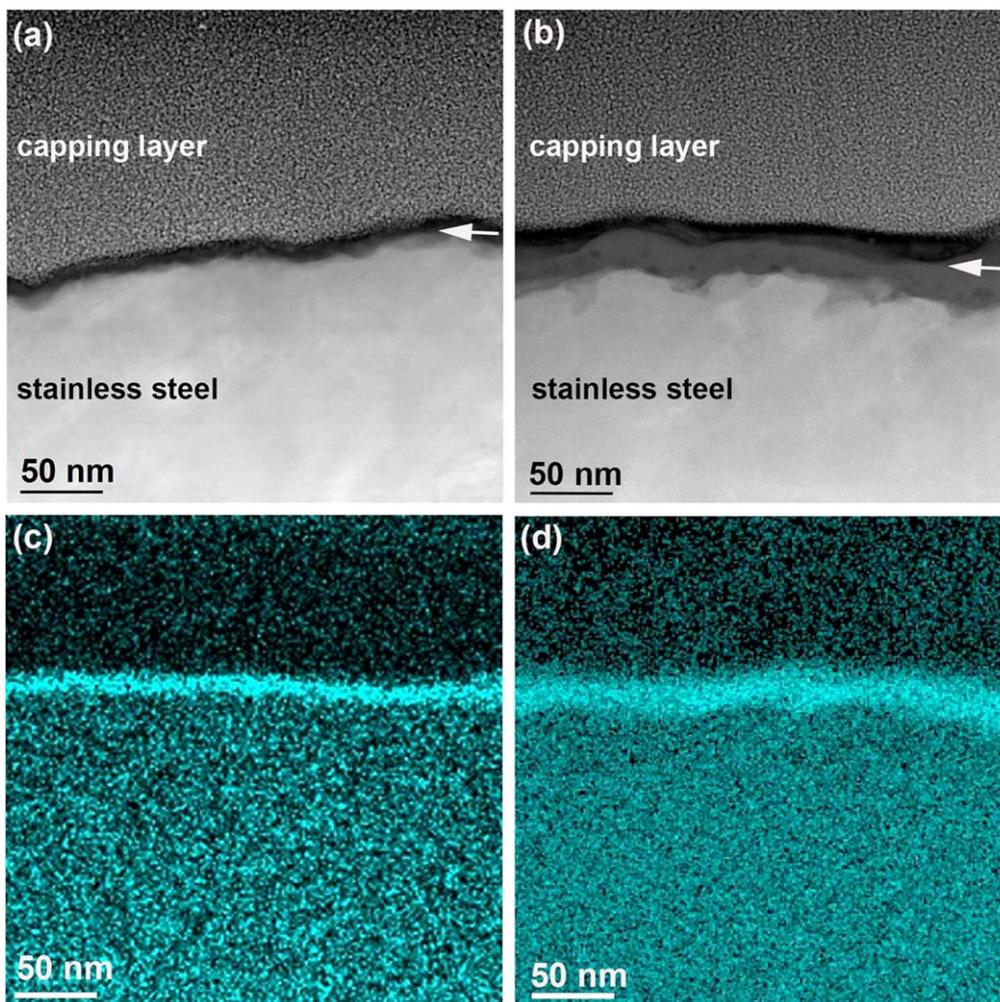
Figure 8. Cross-sectional ADF-SETM images of oxide layers on 316 stainless steel. TEM sample was made by focused ion beams. A Pt capping layer was deposited on surface to protect the oxide layer during the sample making process (a) heat treated at 300 °C for 8 min The white arrow points to the oxide layer (b) heat treated at 600 °C for 1 min (c) an EDS oxygen map of sample (a). (d) an EDS oxygen map of the sample (b).

and 1 min at 600 °C ((b), (d)). The oxide layer as indicated by white arrow is about 10 nm and 30 nm thick respectively. The XPS depth profiles for an unheated and a 300 °C 8 min heated samples are shown in figure 9 where intensities of Cr 2*p*, Fe 2*p* and O 1*s* peaks are plotted against depth. The intensity of each peak is normalized to its maximum value in the depth profile. The depth is obtained by Ar milling rate which is calibrated by TEM. Figure 9(a) indicates that the native oxide of the unheated sample is only about 3 nm thick, and it consists of mostly Cr oxide. The 300 °C 8 min heated sample (figure 9(b)) has about 10 nm thick oxides which contains significant amount of Fe oxides in the top 4 nm then dominated by Cr oxides for the rest of the film.

ρ_c of various samples were measured at 77 and 4.2 K. Unexpectedly the behavior of ρ_c versus pressure cycles a 300 °C 8 min heated sample is very different at 4.2 K from that at 77 K as shown in figure 10(a). While ρ_c decreases slowly with pressure cycling at 77 K, a dramatic ρ_c reduction of almost 4 orders of magnitude is observed at 4.2 K. This measurement was reproduced 3 times. It is conceivable

that for an NI magnet with such a co-wind tape, the magnet properties would change dramatically with load cycles and deviate far from designed values. This would be very problematic. At the end of 30 000 cycles, ρ_c is lower than 100 $\mu\Omega\,cm^2$. Such a low value confirms that the resistivity and thickness of the oxide layer rather than the bulk resistivity of stainless steel dominates ρ_c. Since the contact pressure in an operating NI magnet depends on winding stress, thermal stress, and electromagnetic stress and varies from inner turns to outer turns, it is prudent to investigate the effect of the cycling pressure. Figure 10(b) compares curves of ρ_c versus number of cycles of different pressure of 6, 10, and 25 MPa. The ρ_c was measured at the respective maximum pressure. Although ρ_c reduction is less dramatic with lower pressures, it is still over 2 orders of magnitudes after 30 000 cycles.

ρ_c reduction is much less pronounced in the sample heated at 600 °C for 1 min, as shown in figure 10(c) which also show that the as-received sample behaved similarly to the 300 °C 8 min heated sample.
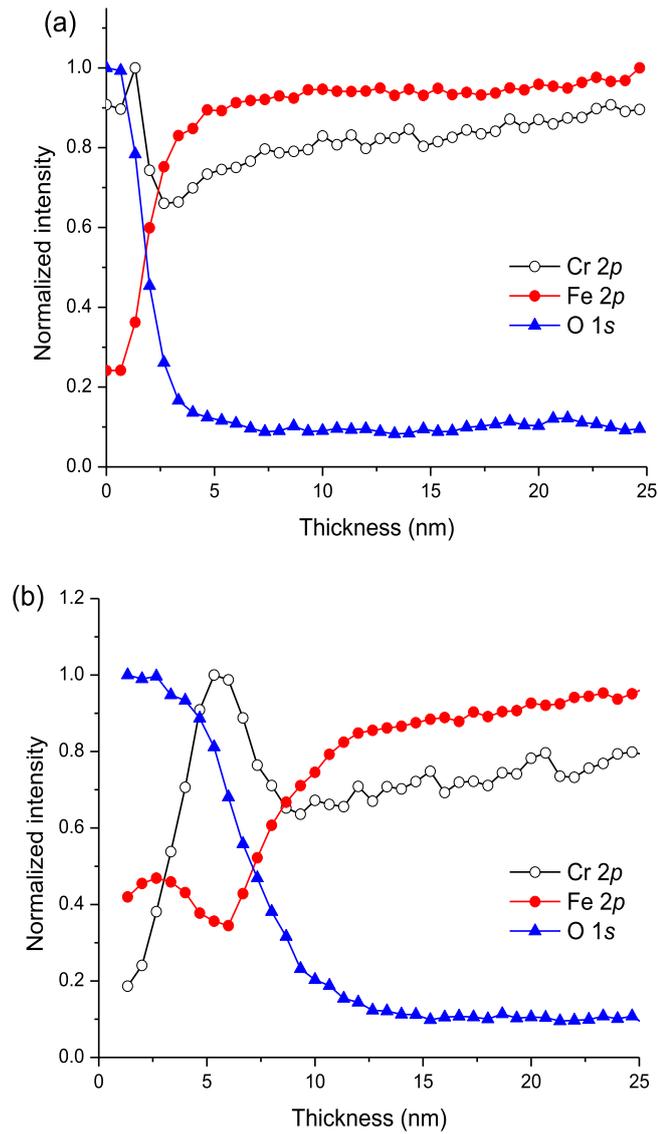
Figure 9. XPS depth profile of surface oxides of 316 stainless steel. Cr 2*p*, Fe 2*p* and O 1*s* were analyzed (a) native oxide, after a few days after 37% HCl etching for 5 min, (b) oxidized by heating at 300 °C for 8 min. The Ar milling rate was calibrated against the thickness measured by TEM.

3.3. Discussions

Due to the considerable uncertainties in the average radius and areal density of asperity spots, it is very difficult to precisely control ρc. Nevertheless a broad ρc control should be possible as demonstrated here by our oxidation experiments of both REBCO surface and the surface of co-winding stainless steel tape. In order to improve the accuracy of ρc control, sophisticated surface characterization and thin film deposition techniques seem to be necessary.

The gradual decrease in ρ_c with load cycling as we observed in Ebonol® C treated REBCO tapes might be associated with wear of the oxide layer. Wear is usually defined as gradual removal of surface materials due to relative motion between two contacting surfaces [32]. In this case, the wear should only occur at the contact asperities. Because the rest of
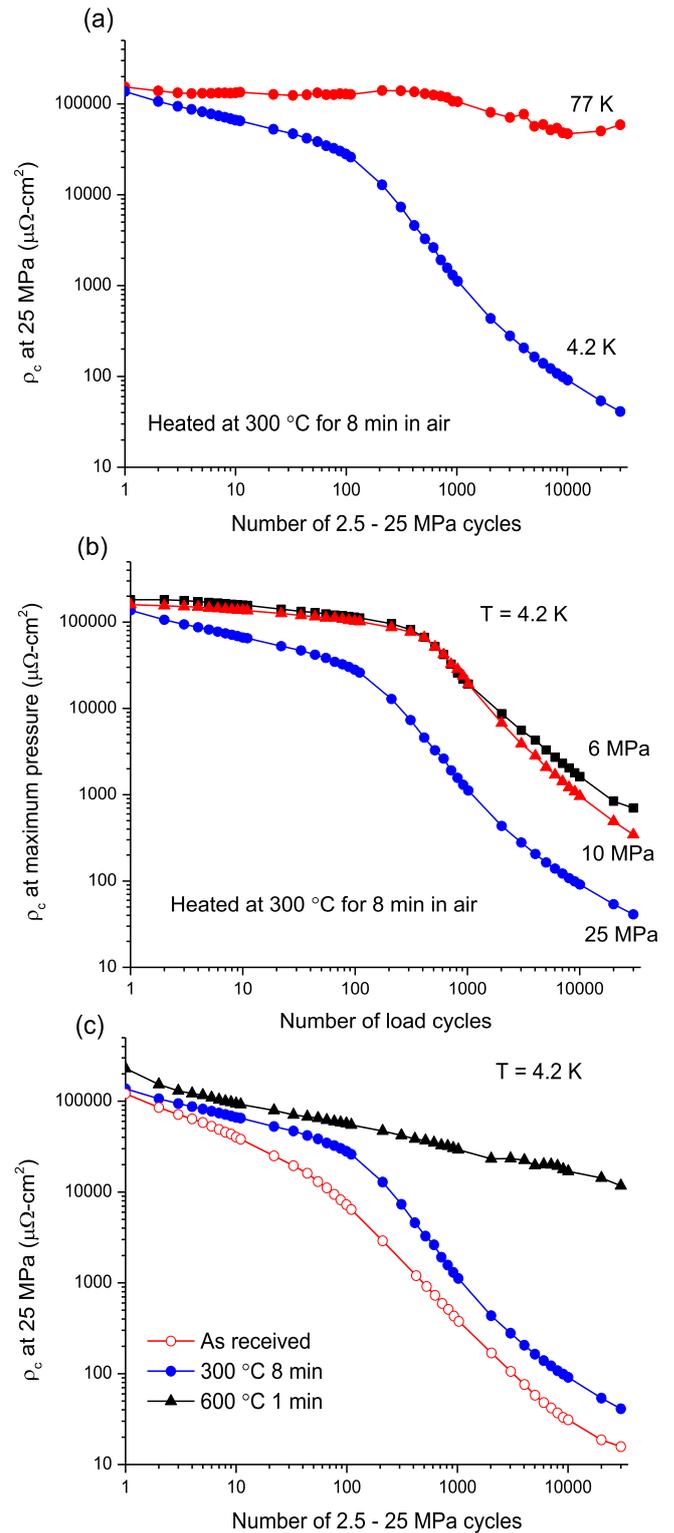
Figure 10. The effect of contact load cycling on ρ_c of 316 stainless steel. (a) The sample was heated at 300 °C for 8 min measured at 77 and 4.2 K. (b) The effect of maximum cycling pressures. ρ_c was measured at the corresponding maximum pressure at 4.2 K. (c) The ρ_c cycling effect of different surface conditions, measured at 4.2 K under 25 MPa pressure.

the sample areas are not actually in physical contact. Although the contract pressure does not create motion in contact plane, it creates a small perpendicular motion. It is conceivable that at contact asperities features on two surfaces are not perfectly

aligned. Under perpendicular pressure, they slide slightly against each other in the loading direction; and the oxide layer is gradually removed by the repeated motions while the debris are retained in the rough interface. The dramatic reduction of ρ_c at 4.2 K with pressure cycles in stainless steel tape heated at 300 °C could also be attributed to the wear of the oxide layer. In order to confirm the wear of the oxide layer at the contact asperities, one has to identify the asperities which is, unfortunately, very difficult. After pressure cycling, the surface of this stainless steel sample was examined by SEM. But contact asperities were not identified. So a 20 μm long cross-sectional TEM specimen was made from this sample by FIB. This TEM experiment were also failed to identify an asperity. The difference in cycling behavior of this sample between 77 and 4.2 K is surprising. It may be speculated that higher thermal stress caused by differential thermal contraction between the oxide and stainless steel at 4.2 K makes the asperity spots more vulnerable to wear. In practice, this means that pressure cycling tests at 77 K does not correlate well with the 4.2 K behavior. So for developing a resistive coating for NI magnets operating at 4.2 K, ρ_c under cyclic pressure might have to be tested at 4.2 K. This dramatic ρ_c reduction did not occur to the sample with about 30 nm oxide formed at 600 °C. This suggests that thicker oxide layer has better wear resistance. It seems that a wear-resistant oxide layer needs to be thicker than 10 nm. Since a 10 nm oxides corresponds to ~100 000 $\mu\Omega\,cm^2$ in ρ_c, a thicker oxide layer would result in a ρ_c of greater than 100 000 $\mu\Omega\,cm^2$. Therefore ρ_c lower than that will be difficult to obtain without suffering from 4.2 K load cycling sensitivity.

4. Conclusions

The control of ρ_c is critical to NI REBCO coil technology. One way to control ρ_c is by controlling the thickness and resistivity of the surface oxides of conductor or co-wind tapes. We used a commercial oxidizing agent Ebonol® C to treat the copper surface of REBCO tapes. The copper oxide layer was characterized by TEM and XPS. The oxide layer grown in Ebonol® C at 98 °C for 1 min is about 0.5 μm of Cu_2O. The ρ_c between two oxidized REBCO is in the order of 35 m$\Omega\,cm^2$ at 4.2 K which decreases slowly with contact pressure cycles. The ρ_c increases but only slightly at 77 K. We also investigated the effect of oxidation of stainless steel co-wind tape on ρ_c in order to control it. The native oxides on 316 stainless steel tape as well as those heated in air at 200 °C–600 °C were examined by TEM and XPS. The native oxides layer is mostly Cr oxides of about 3 nm thick. After heating at 300 °C for 8 min and 600 °C for 1 min, the oxides becomes mostly Fe oxide and its thickness increases to about 10 and 30 nm respectively. For the stainless steel tapes with about 10 nm surface oxides, pressure cycling for 30 000 cycles decreases ρ_c by almost 4 orders of magnitude. Whereas at 77 K, it only changes slightly. For a surface with 30 nm oxide, the ρ_c decreases moderately with load cycles. The results suggest that for an oxidized stainless steel to achieve stable ρ_c over large number of load cycles a relatively thick oxide film is needed.

ORCID iDs

Jun Lu ⓘ https://orcid.org/0000-0001-8521-489X

References

[1] Hahn S et al 2011 IEEE Trans. Appl. Supercond. **21** 1592–5
[2] Yoon S et al 2016 Supercond. Sci. Technol. **29** 04LT04
[3] Kim J et al 2016 IEEE Trans. Appl. Supercond. **26** 4601906
[4] Lécrevisse T et al 2018 Supercond. Sci. Technol. **31** 055008
[5] Markiewicz W D et al 2019 Supercond. Sci. Technol. **32** 105010
[6] Lu J et al 2017 Supercond. Sci. Technol. **30** 045005
[7] Lu J et al 2018 Supercond. Sci. Technol. **31** 085006
[8] Jeong C and Shin S P 2018 Prog. Supercond. Cryog. **20** 15
[9] Bonura M et al 2019 IEEE Trans. Appl. Supercond. **29** 6600305
[10] Holm R 1967 Electric Contacts:Theory and Applications 4th edn (Berlin: Springer)
[11] Slade P G (ed) 2013 Electrical Contacts, Principles and Applications 2nd edn (New York: CRC Press)
[12] Suzuki S et al 1997 Mater. Trans., JIM **38** 1004
[13] Hajimammadov S et al 2018 Surf. Sci. **672-673** 19–22
[14] Parretta A et al 1996 Phys. Status Solidi a **155** 399
[15] Zheng X G et al 1999 Physica C **321** 67–73
[16] Preuss A et al 2018 IEEE Trans. Appl. Supercond. **28** 6601105
[17] MacMahon J D 1949 Composition to blacken surfaces of copper and of alloys containing copper US Patent 2,481,854
[18] Valayil S et al 1985 Solution for forming of black oxide US patent 4,512,818
[19] Sumption M D et al 1999 Cryogenics **39** 197
[20] Meserve R F 1995 Superconductor cable and method of making Patent WO95/27991
[21] Hayase Y et al 2015 Superconducting Wire US patent US 2015.0024.942A1
[22] Lu J and Levitan J W 2019 Rare earth barium copper oxide magnet coils and methods Patent, US 20190267172A1
[23] Markiewicz W D et al 2012 IEEE Trans. Appl. Supercond. **22** 4300704
[24] Tardio S et al 2015 J. Vac. Sci. Technol. A **33** 05E122
[25] Chung O N and Chung S 2003 Vac. Sci. Technol. B **21** 1297
[26] Ferreira M G S et al 2001 Electrochim. Acta **46** 3767–76
[27] Lécrevisse T and Iwasa Y 2016 IEEE Trans. Appl. Supercond. **26** 4700405
[28] Wang Y and Song H 2016 Supercond. Sci. Technol **29** 075006
[29] http://muller.research.engineering.cornell.edu/sites/WEELS/View/Cu_Cu2O.html
[30] Chastain J (ed) 1992 X-Ray Photoelectron Spectroscopy (Eden Prairie, Minnesota USA: Perkin-Elmer Corporation)
[31] Higginson R L et al 2015 Mater. High Temp. **32** 113–7
[32] 1992 Friction, Lubrication and Wear Technology (ASM handbook vol 18) (Cleveland, OH: ASM International)